

Magneto-Optical Properties of Bound Excitons in ZnO

A. V. Rodina,* and M. Strassburg, M. Dworzak, U. Haboeck, A. Hoffmann,
Institute for Solid State Physics, TU Berlin, D-10623 Berlin, Germany

A. Zeuner, H. R. Alves, D. M. Hofmann, B. K. Meyer
I. Physics Institute, Justus-Liebig-University of Giessen, 35392 Giessen, Germany
 (Dated: November 18, 2018)

We present results of magneto-optical measurements and theoretical analysis of shallow bound exciton complexes in bulk ZnO. Polarization and angular dependencies of magneto-photoluminescence spectra at 5 T suggest that the upper valence band has Γ_7 symmetry. Nitrogen doping leads to the formation of an acceptor center that compensates shallow donors. This is confirmed by the observation of excitons bound to ionized donors in nitrogen doped ZnO. The strongest transition in the ZnO:N (I_9 transition) is associated with a donor bound exciton. This conclusion is based on its thermalization behavior in temperature-dependent magneto-transmission measurements and is supported by comparison of the thermalization properties of the I_9 and I_4 emission lines in temperature-dependent magneto-photoluminescence investigations.

PACS numbers: 78.20.Ls, 78.55.-m, 78.40.-q, 71.35.Ji

I. INTRODUCTION

The near band gap photoluminescence (PL) and transmission (PT) spectra of bulk ZnO are known to exhibit a large variety of lines (usually numbered from I_0 to I_{11}) stemming from excitons bound to charged and neutral impurity centers.^{1,2,3,4} Although the origin of these transition lines remained in the focus of intensive research over more than 30 years,^{1,2,3,4,5,6,7,8,9} a convergent picture concerning the nature of the impurities (donor or acceptor character) as well as the symmetry of the valence band hole (Γ_7 or Γ_9 character) involved in the complexes, has not yet emerged.

Bulk ZnO is a direct band gap semiconductor where the valence band maximum is split in a triplet (denoted as A , B and C) by the wurtzite crystal field and spin-orbit interaction. The symmetry of the upper valence subband (A subband) has been the subject of a controversy (Γ_9 or Γ_7 character) for more than 40 years.^{10,11,12,13,14,15,16,17,18,19,20} Based on the polarization properties of the free exciton transitions, most of the authors assumed that the symmetry of the A valence subband in bulk ZnO is Γ_7 ,^{1,2,3,10,11,12,14,15,16,17} in contradiction to most recent studies of the free exciton oscillator strengths (see Ref. 18) and magneto-optical studies of the free A exciton fine structure (see Ref. 19). They were interpreted assuming that the valence band maximum has Γ_9 symmetry. More elaborated theoretical analysis of the exciton fine structure made in Ref. 20, enabled the explanation of the magneto-optical data of Ref. 19 assuming Γ_7 symmetry for the A valence subband. A self-consistent set of the effective mass parameters obtained in the first principles calculations along with the respective structure of the valence band has been used in this analysis.²⁰ The calculated value of the Γ_7 hole effective g factor of $g_h^{\parallel} = -1.3$ in the magnetic field parallel to the c axis ($\mathbf{B} \parallel c$) is close to the value 1.2 assumed in Ref. 19 for the Γ_9 hole but has the opposite sign. On

the contrary, the calculated value of the Γ_9 hole effective g factor $g_h^{\parallel} \approx 3.0$ (see Ref. 20) does not allow to describe the splitting observed in Ref. 19.

Magneto-optical studies are a powerful tool to elucidate the origin of the different bound exciton transitions. The theoretical basis for the description of magneto-optical properties of excitons bound to neutral or charged impurities in hexagonal semiconductors has been developed by Thomas and Hopfield.²¹ The identification of excitons bound to ionized impurities is enabled by the nonlinear splitting of transitions in the magnetic field perpendicular to the c axis ($\mathbf{B} \perp c$). Such splitting governed by the zero field spin-exchange splitting of the corresponding exciton state was indeed observed in ZnO for I_2 and I_3 lines.^{3,4} The transitions from excitons bound to neutral donors ((D^0, X) complex) can be distinguished from the excitons bound to neutral acceptors ((A^0, X) complex) by the thermalization of the absorption or emission components in magnetic field $\mathbf{B} \perp c$. The corresponding thermalization in absorption is caused by the splitting of the ground state (D^0 state) which was observed for the lines from I_5 to I_9 in Ref. 3. An additional proof for the (D^0, X) origin of these lines, as well as of the I_4 line, was obtained by the observation of two electron satellite (TES) PL lines^{5,6,7,8,22,23} that are the transitions to the ($n = 2$) excited state of the neutral donor. However, the authors of Ref. 1 reported on the thermalization of the magneto-PL components in $\mathbf{B} \perp c$ for the lines I_5 to I_{11} . The thermalization in PL is caused by the splitting of the excited state of the acceptor bound exciton complex. Therefore, an attribution of these lines I_5 to I_{11} to (A^0, X) complexes was given in Ref. 1. This is in contradiction to the magneto-absorption data of Ref. 3. Moreover, from the thermalization of PL components in magnetic field $\mathbf{B} \parallel c$ the authors of Refs. 1 concluded that the Zeeman splitting of the hole in the acceptor ground state was larger than the Zeeman splitting of the electrons. This contradicts strongly to the results

reported previously in Ref. 2 for the g values of the Γ_7 holes involved in the same transitions. Thus, the nature of the neutral bound exciton transitions, the symmetry of the holes and the reliable hole g values are up to now not clear.

In the present work, we report in detail on theoretical and experimental studies of the magneto-optical properties of shallow bound excitons in ZnO. We take into account all possible configurations of bound exciton complexes involving holes of Γ_9 and Γ_7 symmetry with different signs and values of the hole g factors. For each configuration we analyze the selection rules for the optical transitions and calculate the magnetic field dependencies of the transition energies in $\mathbf{B} \parallel c$ and $\mathbf{B} \perp c$ geometry as well as their dependence on the angle between the magnetic field and the c axis (angular dependence). The analysis of the polarization properties and angular dependencies of the magneto-PL transitions in the nominally undoped and nitrogen doped ZnO crystals allows us to reveal the symmetry and the g values of the valence band holes. This enable us further to analyze the thermalization properties of the magneto-PL and magneto-absorption components in magnetic field perpendicular and parallel to the c axis in order to reveal the nature of the neutral impurity centers.

The paper is organized as follows. Section II describes a the experimental conditions and the investigated samples. In Section III we report on the zero field PL and PT investigations in ZnO and discuss the Zeeman splitting of the observed transitions in terms of excitons bound to ionized impurity centers (see Section III A) and of excitons bound to neutral impurities centers (see Section III B). The thermalization properties of the excitons bound to neutral impurities are discussed in Sec. IV. In Section V we discuss our results in terms of the literature. The main results are summarized in Section VI.

II. EXPERIMENTAL SETUP AND SAMPLES

We used nominally undoped (as grown from Eagle-Picher, see for details Ref. 23) and nitrogen doped bulk ZnO crystals. A nitrogen doped ZnO sample was prepared from the as grown one by ion implantation (2 MeV, 10^{13} cm^{-2}) followed by a thermal annealing process at 900° C for 15 minutes (see also Ref. 23).

The magneto-PL measurements were performed at liquid helium temperature in a split-coil magneto cryostat allowing the variation of both temperature (2 – 300 K) and magnetic field (0 – 12 T). Photoluminescence was excited by the 325 nm line of a HeCd laser. A 450 W XBO lamp was used as excitation source for the transmission investigations. The spectral resolution of the detection system was better than 0.15 meV.

The magneto-PL and magneto-PT measurements were performed in Faraday configuration (magnetic field \mathbf{B} parallel to the c axis of the crystal and parallel to the \mathbf{k} -vector of the detected light) and in Voigt configuration

($\mathbf{B} \perp c \parallel \mathbf{k}$). Additionally, the angles between \mathbf{B} and c axes were varied from 0 to 90 degrees at fixed magnetic field of 5 T. The circular polarization of the light (σ^+ and σ^-) in the Faraday configuration was analyzed using $\lambda/4$ plate and linear polarizer. Additionally, PL spectra with $\mathbf{B} \parallel c$, $\mathbf{k} \perp c$ and the electric field vector of the luminescence light $\mathbf{E} \parallel c$ were recorded for the ZnO:N specimen. Thermalization behavior of the Zeeman split components of the emission and transmission lines was revealed by temperature-dependent measurements in the Faraday and Voigt configurations.

III. ZEEMAN BEHAVIOR OF THE BOUND EXCITON COMPLEXES

The zero field PL (solid line) and PT (dashed line) spectra of the as grown (nominally undoped) ZnO and nitrogen doped ZnO:N are shown in Figure 1 (a) and (b), respectively. The strongest lines in the as grown ZnO (see Fig. 1 (a)) are the I_4 (368.72 nm or 3.3628 eV) and the overlapping transitions attributed to I_7 (368.90 nm or 3.3600 eV) and I_8 (368.92 nm or 3.3598 eV). Additionally, lines with lower intensity are detected between I_4 and I_7/I_8 . The weak line I_9 (369.27 nm or 3.3567 eV) is observed both in PL and PT spectra. Following the Refs. 22,23, we attribute the I_4 transition as an exciton bound to a neutral shallow H donor that can be easily removed by an annealing process.^{22,23} Indeed, the I_4 PL line is absent in ion implanted ZnO:N (see Fig. 1 (b)). This is because of the post annealing processes at 900° C included in the doping procedure. The PL spectrum of ZnO:N is dominated by two lines: a new line I_2 (368.07 nm or 3.3676 eV) and the I_9 transition. The latter considerably gains in intensity in PL as well as in PT spectra compared to the undoped ZnO and becomes the strongest transition in ZnO:N. An additional transition (labeled I_{9a}) on the low-energy tail of the I_9 line in ZnO:N can be seen in the PT spectra that was not resolved by the PL measurements and was not observed in the undoped ZnO crystals. The wavelengths of the lines (given here in air with an accuracy of 0.02 nm) coincide with the wavelengths and labeling of the lines used in Refs. 1,2,3,4.

In Figure 2 the magneto-PL spectra from I_2 to I_9 for the ZnO:N are shown in Faraday configuration (a), Voigt configuration (c) and for the different angles between the magnetic field direction and the c axis at $B = 5 \text{ T}$ (b). The most important feature of the spectra in Figures 2 (b) and (c) is a rising new transition line at an energy about 1 meV below I_2 . This I_3 transition (368.19 nm or 3.3666 eV in zero field), that is forbidden in $\mathbf{B} \parallel c$, $\mathbf{E} \perp c$ geometry, has been also observed in parallel magnetic field with the light polarized along the c axis ($\mathbf{E} \parallel c$ configuration). Such behavior allows us unambiguously to identify the I_2 and I_3 transition as originating from excitons bound to an ionized impurity (see a detailed discussion in the Subsection A), while the other transi-

tions that show a linear Zeeman splitting in $\mathbf{B} \perp c$ will be assigned to excitons bound to neutral impurities (see Subsection B).

A. Exciton bound to an ionized impurity

Let us consider in details the magnetic field and angular dependencies of the emission lines I_2 and I_3 generated by excitons bound to an ionized impurity. These dependencies allow us to determine the symmetry and the g values of the valence band hole involved in the corresponding bound excitons. In Figure 3 we sketch all possible transitions with selection rules corresponding to our observations for I_2/I_3 lines in Fig. 2. We consider the holes from the Γ_7 (case (a)) and Γ_9 (case (b)) valence bands. The zero field exchange splitting between the Γ_1 and Γ_2 exciton states is neglected in Fig. 3 (a) as it is known to be small in ZnO.²⁰ The magnetic field $\mathbf{B} \parallel c$ linearly splits the I_2 transition (allowed in $\mathbf{E} \perp c$ configuration) as well as the I_3 transition (allowed in $\mathbf{E} \parallel c$ configuration). The upper-energy component of the I_2 line is active for the right-circular polarized light σ^+ (see dashed line in Fig. 2 (a)). The perpendicular magnetic field ($\mathbf{B} \perp c$) mixes the exchange-split exciton states: Γ_5 state with Γ_1/Γ_2 states in the case(a) in Fig. 3 or with Γ_6 state in the case (b). The resulting high- and low-energy components of I_2/I_3 remain nearly unsplit in $\mathbf{B} \perp c$ and their energy dependencies on the magnetic field are mostly determined by the zero field splitting. Four transition components can be distinguished for an arbitrary angle between the direction of the magnetic field and the c axis. The magnetic field dependencies of the transition energies in Faraday and Voigt configurations and their angular dependence at $B = 5$ T are shown in Figure 4.

The linear splitting of the I_2 line in $\mathbf{B} \parallel c$ can be described as $\mu_B B g_{exc}$ with the exciton effective g -factor $g_{exc} = 0.71$, where μ_B is the (positive) value of the Bohr magneton. In the case (a), where a hole of Γ_7 symmetry is involved, we have $g_{exc} = g_e + g_h^{\parallel}$. Here $g_e \approx 1.95$ is the electron (isotropic) effective g factor and g_h^{\parallel} is the hole effective g factor in magnetic field parallel to the c axis.²⁴ In the case (b) we have $g_{exc} = g_h^{\parallel} - g_e$ for a hole of Γ_9 symmetry. Since $g_{exc} > 0$, we may assume a negative effective g factor $g_h^{\parallel} < 0$, $|g_h^{\parallel}| < g_e$ for the hole of Γ_7 symmetry or $g_h^{\parallel} > g_e$ for the hole of Γ_9 symmetry. We use the theoretical expressions obtained in Ref. 21 for the angular dependence of the transition energies in Fig. 4. From fitting the angular dependence and the Zeeman splitting of the I_3 line in $\mathbf{B} \parallel c$ it follows that $|g_h^{\parallel}| < g_e$. For comparison, the dependencies calculated with $|g_h^{\parallel}| < g_e$ and with $|g_h^{\parallel}| > g_e$ are shown in Fig. 4 by solid curves and dashed curves respectively. Since $|g_h^{\parallel}| < g_e$, we see that the observed transitions involve a hole of Γ_7 symmetry as shown in Figure 3 (a). This

demonstrates that the hole in the lowest exciton state and thus the upper A valence subband in ZnO also have Γ_7 symmetry.

The values of the electron and hole effective g factors obtained from the fitting procedure (shown by solid curves) in Fig. 4 are: $g_e = 1.95$, $g_h^{\parallel} = -1.24$ and $g_h^{\perp} = 0.1$. The value of the zero-field spin-exchange splitting between the Γ_5 exciton state (I_2 transition allowed with the circular polarized light) and the Γ_1/Γ_2 exciton states (I_3 transition allowed with $\mathbf{E} \parallel c$) is 0.98 meV in a good agreement with Refs. 4,20,25. The zero field splitting between Γ_1 and Γ_2 exciton states was neglected. The Zeeman splitting of the I_3 line in $\mathbf{B} \parallel c$, however, could be fitted more accurately if one assumed the splitting between the Γ_1 and Γ_2 states to be about 0.1 – 0.2 meV. A limited spectral resolution in the $\mathbf{k} \perp c$, $\mathbf{E} \parallel c$ configuration did not allow us to evaluate this splitting more precisely.

The stability of the (D^+, X) or (A^-, X) complex in semiconductors depends strongly on the ratio of electron and hole effective masses.²⁶ In the case of ZnO, the single band isotropic mass approximation predicts the existence of the excitons bound to ionized donors.²⁵ Next, the presence of acceptors in the ZnO:N may induce the ionization of the shallow donors²⁷ as in the case of Li and Na doped ZnO.⁴ Therefore, we attribute the I_2 and I_3 lines in the doped ZnO:N to transitions of excitons bound to respective ionized donors $((D^+, X_A(\Gamma_7))$ complex).

B. Excitons bound to neutral impurities

The behavior of the emission lines from I_4 to I_9 in $\mathbf{B} \perp c$ is different from that of the I_2/I_3 lines. Their linear Zeeman splitting indicates transitions originating from excitons bound to neutral impurities. In Figure 5 we sketch all possible transitions for such complexes corresponding to our observations in Fig. 2. In the case of a donor bound exciton complex (Fig. 5 (a) and (b)), the spins of two electrons are anti-parallel and the Zeeman splitting of the excited (D^0, X) state is determined by the anisotropic hole effective g factor (g_h), while the splitting of the ground D^0 state is given by g_e . In the case of an acceptor bound exciton complex (Fig. 5 (c) and (d)), two holes have the same symmetry and anti-parallel spins. Hence, the splitting of the excited (A^0, X) state is determined by g_e , while the ground A^0 state splits according to g_h . For all transitions from I_4 to I_9 the observed Zeeman splitting in $\mathbf{B} \parallel c$ is less than the Zeeman splitting of the electrons. Furthermore, the upper Zeeman split energy components of all transitions are active in σ^+ polarization. Both of these facts can be explained in the framework of our conclusion that the ground state hole has Γ_7 symmetry with $g_h^{\parallel} < 0$, $|g_h^{\parallel}| < g_e$. The corresponding ordering of the hole sublevels in parallel and perpendicular magnetic fields and optically active transitions in $\mathbf{E} \perp c$ configuration are shown in Fig. 5 (a) and (c). For the sake of completeness, we consider also the Γ_9 hole with

$g_h^{\parallel} > g_e$ (see Fig. 5 (b) and (d)). The respective transitions involving holes from the B valence subband may be observed in PL spectra at higher temperatures^{22,23} or in the transmission spectra.

For a further insight, we discuss the emission lines I_9 and I_4 in detail. These lines represent the dominant recombination in ZnO:N and as grown ZnO bulk crystals, respectively, and are spectrally resolved from the other observed emission lines. The Zeeman behavior of these two lines is very similar. The transitions allowed for $\mathbf{E} \perp c$ split linearly as function of magnetic fields parallel and perpendicular to the c axis. Four transition components can be distinguished for an arbitrary angle between the direction of the magnetic field and the c axis. The B -field dependencies up to 5 T of the I_4 transition energies in $\mathbf{B} \parallel c$ and $\mathbf{B} \perp c$ as well as the angular dependence at $B = 5$ T are shown in Figure 6. The corresponding B -field and angular dependencies of the I_9 line in ZnO:N are shown in Figure 7. Additionally, we also show the results of the PT measurements for ZnO:N and of the PL measurements for as grown ZnO in Fig. 7.

According to Ref. 21, the magnetic field dependence of the transition energies and the absolute value of the hole anisotropic g factor are given by $\pm 1/2\mu_B B(g_e \pm g_h)$ and $g_h = \sqrt{|g_h^{\parallel}|^2 \cos^2 \Theta + |g_h^{\perp}|^2 \sin^2 \Theta}$, respectively, where Θ is the angle between the c axis and the direction of the magnetic field. The analysis of the angular dependence shows that an excellent agreement between experimental data and theoretical modeling is possible if and only if we assume that the hole g factor is smaller than electron's g factor: $|g_h^{\parallel}| < g_e$. This conclusion follows from a comparison of the angular dependencies calculated with $|g_h^{\parallel}| < g_e$ (solid curves) and with $|g_h^{\parallel}| > g_e$ (dashed curves) in Figures 6 and 7. The values of the electron and hole effective g factors used for the fitting (solid curves) are $g_e = 1.97$, $g_h^{\parallel} = -1.21$ and $g_h^{\perp} = 0.1$ for the I_4 and $g_e = 1.86$, $g_h^{\parallel} = -1.27$ and $g_h^{\perp} = 0.06$ for the I_9 line. We note that only the data for I_9 PL line in ZnO:N are used for the fitting procedure in Fig. 7. Since g_h^{\perp} is small, it is neither possible to resolve a respective additional splitting of the transitions in $\mathbf{B} \perp c$ nor to observe the nonlinear behavior of the dependence of the transition energies on $\cos \Theta$ indicating the holes of the Γ_7 symmetry.³ Nevertheless, the Γ_7 symmetry of the holes is unambiguously established by the analysis presented above.

Now, we have found on one hand that the Zeeman behavior of the I_9 lines in ZnO and ZnO:N is identical (see Fig. 7) and very similar to the Zeeman behavior of the I_4 line in as grown ZnO. The values of g_h^{\parallel} derived for I_4 and I_9 are very close to the $g_h^{\parallel} = -1.24$ obtained in the Subsection A for the hole involved in the exciton bound to ionized donor and to the g factor of the hole in 1S free exciton state.^{15,16,17,20} On the other hand, one may expect the g_h^{\parallel} values of the holes involved in the acceptor bound exciton transitions to differ significantly from the g values of the holes involved into excitons bound to ion-

ized or neutral donors as it was found in CdS.²¹ Indeed, the expected value of the Γ_7 hole g factor in a shallow acceptor ground state in ZnO is about -0.75 ± 0.05 .²⁸ This makes us to assume that both I_4 and I_9 transitions are rather to be assigned to the $(D^0, X_A(\Gamma_7))$ than to the $(A^0(\Gamma_7), X_A(\Gamma_7))$ complexes. To support this assumption, we analyze the thermalization properties of the I_4 and I_9 lines in the next Section.

We have observed very similar Zeeman behavior for the less intensive lines between I_4 and I_9 with the values of the electron and hole effective g factors in the range of $g_e = 1.92 \pm 0.06$, $g_h^{\parallel} = -1.24 \pm 0.04$ and $g_h^{\perp} = 0.08 \pm 0.04$. The Zeeman splitting of the hole states is found to be always smaller than the splitting of the electron states. From the polarization properties it follows then that all observed PL transitions involve the Γ_7 holes from the A valence subband. For the hole of Γ_9 symmetry from the B valence subband the splitting in the parallel magnetic field is predicted to be larger than those of the electron.²⁰ This would lead to the crossing of the transition energies at an angle around 40° as shown by dashed lines in Figs. 6 and 7. Since we do not observed such a crossing, we can not associate any transition with the holes of Γ_9 symmetry. We conclude therefore, that the excited states of the complexes involving holes from the B valence subband do not make major contribution to the low temperature PL.

IV. THERMALIZATION PROPERTIES OF EXCITONS BOUND TO NEUTRAL IMPURITIES

The knowledge of the Γ_7 hole effective g factors obtained in the previous Section allows us to predict the respective thermalization properties of the Zeeman split components in magnetic fields parallel and perpendicular to the c axis (see Figure 5 (a) and (c)). We recall, that the thermalization behavior of the absorption components depends on the splitting of the ground (D^0 or A^0) state of the respective complex. In a contrary to that, the thermalization of the PL components is caused by the splitting of the complex excited state, (D^0, X) or (A^0, X) respectively. Since g_h^{\perp} of the Γ_7 hole is small, a distinct allocation of the observed transitions either to a neutral acceptor or to a neutral donor exciton complex in ZnO, similar to the situation in CdS,²¹ can be facilitated by thermalization properties in $\mathbf{B} \perp c$.

Thermalization properties in transmission

According to Fig. 5 (c), the intensities of the $A^0(\Gamma_7) \rightarrow (A^0(\Gamma_7), X(\Gamma_7))$ transitions are expected to be equal in $\mathbf{B} \perp c$. In contrast, the intensity of the low-energy component of the $D^0 \rightarrow (D^0, X(\Gamma_7))$ transitions in $\mathbf{B} \perp c$ should be less than that of the high-energy component at low temperatures and should increase with temperature. The opposite behavior for the

$A^0(\Gamma_7) \rightarrow (A^0(\Gamma_7), X(\Gamma_7))$ (case (c) in Fig. 5) and $D^0 \rightarrow (D^0, X(\Gamma_7))$ (case (a) in Fig. 5) transitions is expected in $\mathbf{B} \parallel c$ too. Since $|g_h^\parallel| < g_e$, the intensity of the low-energy component at low temperatures in $\mathbf{B} \perp c$ should be less or more than that of the high-energy component in the cases (a) or (c) respectively. The intensity of the low-energy component (high-energy component) should increase with temperature in the case of donor bound exciton (acceptor bound exciton) complexes.

Temperature-dependent transmission spectra were recorded for magnetic fields up to 5 T. The absorption of the I_9 line was revealed in both samples. In the ZnO:N the additional absorption peak I_{9a} appeared. However, we focus here only on the main I_9 absorption peak in ZnO:N. The magnetic field and angular dependencies of this absorption peak derived from PT spectra (see Fig. 7) confirm that it has the same origin as the I_9 PL line. Unfortunately, we were not able to detect the absorption peak corresponding to the PL I_4 line in as grown ZnO. Instead, we observed an increase of the detected light intensity at the respective energy (see Fig. 1 (a)) probably caused by the strong emission processes.

The thermalization properties of the absorption line I_9 for $\mathbf{B} \perp c$ at 2 T (solid curves) and at 3 T (dashed curves), and for $\mathbf{B} \parallel c$ at 5 T are depicted in Figure 8 (a) and (b), respectively. The observed temperature behavior of the low-energy and high-energy absorption components of the I_9 for $\mathbf{B} \perp c$ and $\mathbf{B} \parallel c$ is in complete agreement with the expected behavior of the $D^0 \rightarrow (D^0, X(\Gamma_7))$ transitions as described above. The intensity ratio of the low-energy and the high-energy Zeeman split components decreases with increasing magnetic fields (due to the respective increase of the Zeeman splitting of the initial D^0 state) and increases with increasing temperatures. Therefore, we attribute the I_9 line as a donor bound exciton complex in an excellent agreement with magneto-absorption data of Ref. 3.

Thermalization properties in emission

Although the I_9 transition in nominally undoped ZnO single crystals was assigned to a donor bound exciton complex in Ref. 3), in more recent publication of Ref. 1 this line was attributed to an acceptor bound exciton. The latter conclusion was based on the thermalization behavior of the PL components in $\mathbf{B} \parallel c$.¹ Indeed, in PL measurements the thermalization properties are determined by the splitting of the excited state of the complex. Therefore, the intensities of the $(D^0, X(\Gamma_7)) \rightarrow D^0$ transitions (see Fig. 5 (a)) are expected to be equal in $\mathbf{B} \perp c$, while the intensity of the low-energy component of the $(A^0(\Gamma_7), X(\Gamma_7)) \rightarrow A^0(\Gamma_7)$ transitions (see Fig. 5 (c)) in $\mathbf{B} \perp c$ should be less than that of the high-energy component at low temperatures and should increase with rising temperature. However, since $|g_h^\parallel| < g_e$, the same or the opposite intensity relation should be also observed in $\mathbf{B} \parallel c$ in the case of $(A^0(\Gamma_7), X(\Gamma_7)) \rightarrow A^0(\Gamma_7)$ or

$(D^0, X(\Gamma_7)) \rightarrow D^0$ transition, respectively. To verify the self-consistence of the PL results, we also analyze the thermalization properties of the I_9 and I_4 PL lines for $\mathbf{B} \perp c$ and $\mathbf{B} \parallel c$.

For $\mathbf{B} \perp c$, we have found that the intensity of the low-energy PL component of the I_9 line in ZnO:N is stronger than that of the high-energy component (see Fig. 9 (a)). This was predicted for an acceptor bound exciton (see Figure 5 (c) and (d)). On a first glance, this contradicts the respective results of the transmission experiments presented above, but is in good agreement with Refs. 1,2. However, we did not observe this effect for the I_9 PL line in as grown ZnO where the intensity ratio of both component was independent of the temperature as well as of the magnetic field value. For $\mathbf{B} \parallel c$, the temperature behavior of the PL components of the I_9 for as grown ZnO and ZnO:N is in an excellent agreement with the expected behavior of the $(D^0, X_A(\Gamma_7)) \rightarrow D^0$ transitions with $|g_h^\parallel| < g_e$ (see Fig. 5 (a)). The low-energy Zeeman component exhibits less intensity in $\mathbf{B} \parallel c$ (see Fig. 9(b)). Its intensity increases with increasing temperatures. In contrast to that, the high-energy PL component would to be expected weaker for the $(A^0(\Gamma_7), X_A(\Gamma_7)) \rightarrow A^0(\Gamma_7)$ transitions (see Figure 5(c)). But this was not observed. Therefore, we conclude that the PL results for the I_9 line in ZnO:N for $\mathbf{B} \perp c$ and $\mathbf{B} \parallel c$ contradict each other. Taken alone they do not allow an unambiguous assignment of the bound exciton complex.

We have detected a very similar controversial thermalization behavior of the I_4 PL line (see Figure 10). For $\mathbf{B} \perp c$ at low temperatures (Fig. 10 (a)), a stronger intensity was recorded for the low-energy Zeeman split component contradicting to a donor-bound exciton complex. Although for $\mathbf{B} \parallel c$ (Fig. 10 (b)) the low-energy component was stronger (as it is expected for an acceptor bound exciton), its intensity increased with increasing temperatures as it would be typical for a donor bound exciton.

As the PL results for the I_9 and I_4 lines are similar, we assign both the I_9 and I_4 transition to the donor bound exciton complex on the basis of the self-consistent thermalization behavior of I_9 in transmission spectra. An explanation of the controversial temperature behavior of the PL components observed for $\mathbf{B} \perp c$ can be, for example, attributed to the light re-absorption process or to another energy transfer mechanism. It is necessary to note that the thermalization behavior corresponding to the (D^0, X) complex was not observed for the I_4 in Ref. 3. This was probably caused by the same processes that prevented our observation of the I_4 transition in PT spectra at all.

V. DISCUSSION

In this section we discuss our identification of the observed emission lines and compare with those known from the literature. We also evaluate possible candidates for

generating the nitrogen bound exciton transition in the ZnO:N crystals.

I₂ and I₃ lines

We attributed the I_2 and I_3 emission lines observed in ZnO:N to transitions from the exchange split states of the $(D^+, X(\Gamma_7))$ complex. The formation of the ionized donor bound exciton complex is caused by the N doping in the same way as by the Na and Li doping in ZnO:Na and Zn:Li, respectively. The value of 0.98 meV obtained for the zero field spin-exchange is close to 0.9 meV reported in Ref. 4 for the same lines and to the theoretical calculations of Ref. 25. However, the authors of Ref. 4 assumed another valence band ordering with the Γ_9 symmetry of the top valence subband and thus assigned the I_2 and I_3 lines to the $(D^+, X(\Gamma_9))$ complex. The field dependence of the transition energies in $\mathbf{B} \parallel c$ and their angular dependence at $B = 4.5$ T were fitted in Ref. 4 by using $g_h^\parallel = 1.5$ for the Γ_9 hole. This would correspond to $g_{exc} = g_h^\parallel - g_e < 0$ and, as one can see from the scheme in Fig. 4 (b), to the σ^- polarization of the upper-energy Zeeman split component of the I_2 transition. This contradicts to our observations in Fig. 2 (a).

In Ref. 3, the absorption lines I_{c1} (3.368 eV) and I_{c2} (3.367 eV), corresponding to the emission lines I_2 and I_3 , respectively, were assigned to the different (D^+, X) complexes: I_{c1} to the $(D^+, X_A(\Gamma_7))$ complex while I_{c2} to the $(D^+, X_B(\Gamma_9))$ complex. The latter represents the excited state of the exciton bound to the charged donor and indeed could be observed in absorption. However, the energy separation between I_{c1} and I_{c2} absorption lines is close to the 0.98 meV spin-exchange splitting of the $X_A(\Gamma_7)$ exciton obtained in the present work and much smaller than the separation of the A and B valence subbands (4.5 meV^{22,23}). Therefore, we assume that the absorption lines I_{c1} and I_{c2} in Ref. 3 originate from the Γ_5 and Γ_1/Γ_2 states of the $(D^+, X_A(\Gamma_7))$ complex. The preferred polarization $\mathbf{E} \parallel c$ of the I_{c2} transition reported in Ref. 3 agrees with this assumption, too.

I₄ line

The I_4 is known to stem from an exciton bound to a shallow donor.^{6,7,22,23} A strong evidence of the donor bound exciton complex origin of the I_4 line is given by the observation of TES transitions.^{7,8,22,23} The binding energy of the donor is determined to be about 46 meV.^{22,23} Annealing annihilates this shallow donor and thus neither I_4 line nor the respective TES transition can be observed in the annealed samples. Correlated by temperature-dependent Hall effect measurements²² and the magnetic resonance experiments²⁹ this particular donor was attributed to Hydrogen.^{22,23} Our zero field PL measurements for the as grown ZnO and for the ZnO:N, whose

preparation conditions included an annealing process, confirmed this correlation³⁰ and thus the (D^0, X) origin of the I_4 line.

We did not detect the I_4 line in PT spectra and thus could not obtain a direct evidence for its donor bound exciton nature from our magneto-transmission studies. Nevertheless, the observed Zeeman splitting of the I_4 PL line is an excellent agreement with the model of the $(D^0, X(\Gamma_7))$ complex. The obtained value of the Γ_7 hole effective g factor is typical for the holes in excitons bound to ionized or neutral donors in ZnO. We note, for example, that in CdS the g values were found to differ significantly for the holes in excitons bound to shallow donors from the holes in shallow acceptor states.²¹ The thermalization behavior of the I_4 PL line is very similar to those of the I_9 line whose (D^0, X) origin was confirmed directly by the magneto-PT studies.

I₉ line

Our assignment of the I_9 line to the donor bound exciton complex is based on the thermalization properties in absorption in an excellent agreement with Ref. 3. Taking into account the re-absorption process in the bulk crystals, our PL results as well as the PL results reported in Refs. 1,2 can be also explained within the $(D^0, X(\Gamma_7))$ model. Similar to the case of the I_4 line, we additionally support the allocation of the I_9 line to the donor bound exciton by the observation of the TES transitions in ZnO:N. These transition appear at energy about 50 meV below the I_9 line in zero field PL spectra,³⁰ which corresponds to the donor binding energy of about 63 meV. Recently, the TES transitions for the I_9 line was likewise observed in nominally undoped ZnO⁷ and in ZnO:Na and ZnO:Li single crystals.²³

Previously, the I_9 line in ZnO:Na and ZnO:Li crystals was associated with sodium acceptors.³¹ However, this assignment is in conflict to the recent observation of TES transitions.²³ We have found in the present work that the intensity of the I_9 PL and absorption transitions increase significantly in ZnO:N in comparison with undoped bulk crystals. The same Zeeman behavior and the identical energy positions in as grown ZnO and doped ZnO:N crystals prove that this line has the same origin. One could then associate this line with excitons bound to a N acceptor in ZnO:N. However, our identification of this line as a donor bound exciton complex excludes such assignment.

It is worth to note, that the I_9 line was reported not to gain in intensity upon the annealing processes at temperatures up to 850° C.^{22,23} However, secondary ion mass spectroscopy experiments showed that In was unintentionally introduced into the ZnO:N upon implantation and annealing at 900° C. In diffusion experiments performed quite recently showed that the 3.357 eV I_9 line could be indeed caused by the indium donor.²³

Do we observe the nitrogen bound excitons in ZnO:N ?

Previous publications have shown that nitrogen on an oxygen site acts as an acceptor with a binding energy of about 165 meV.^{27,32,33} PL studies on nitrogen doped ZnO layers showed that nitrogen leads to a at 3.359 eV within an accuracy of 1 meV.³⁴ In this spectral range we have detected the strongest intensity for the I_7 line in ZnO:N. The I_{6a} , I_7 and I_8 lines show similar Zeeman behavior in comparison to I_4 and I_9 that is typical for the donor bound exciton complexes. However, since the energy differences of the lines I_{6a} , I_7 and I_8 are very small, a comprehensive evaluation of magnetic field dependence and thermalization properties is very difficult and partly prevented by the linewidth (FWHM) of the Zeeman split components.

In the following, two other possible candidates for the nitrogen bound exciton are introduced and discussed. First, the I_{9a} absorption peak appeared on the low-energy tail of the I_9 in the PT spectra of ZnO:N (see Figs. 1 and 8). We emphasize that this peak was not observed in the as grown undoped ZnO as well as in annealed undoped ZnO.³⁰ However, we do not have a clear evidence of its acceptor bound exciton origin. Its position close to the I_9 line, weak intensity and the large half width (FWHM) prevents consequent conclusions about its thermalization properties in transmission.

The last potential candidate for the nitrogen bound exciton transition is a new weak line located about 2 meV above the I_9 transition in the PL spectra of ZnO:N (see the line labeled as I_9^* in Fig. 1 (b)). This line was too weak both in PL and transmission to perform the magneto-optical studies. We note however, that more likely this line is to be attributed to an excited rotator state of the I_9 donor bound exciton complex. This is in agreement with the calculated position of such state in Ref. 23 and the excitation measurements of Ref. 1. In a

similar way, the weak transition located about 1.1 meV above I_4 in as grown ZnO (the line labeled as I_4^* in Fig. 1 (a)) may be attributed to the excited rotator state of the I_4 donor bound exciton complex.

VI. CONCLUSION

In summary, experimental and theoretical magneto-optical studies on undoped and nitrogen doped bulk ZnO facilitated new insights of the valence band ordering, hole g values, and of the nature of shallow bound exciton complexes. The Γ_7 character of the upper valence band was derived according to polarization properties and angular dependence in magnetic field of excitons bound to charged and neutral impurity centers. Hence, the valence band A , B and C pose the Γ_7 , Γ_9 and Γ_7 symmetry, respectively. The obtained Γ_7 hole effective g value in parallel field of -1.24 ± 0.04 is in a good agreement with theoretical calculations.²⁰ We observed no PL transitions involving the Γ_9 hole states.

The presence of ionized donors confirmed the formation of acceptors in ZnO:N. However, an unambiguously allocation of the nitrogen impurity center to one of the observed bound exciton lines was not possible. The dominant recombination lines, I_9 in ZnO:N and I_4 in as grown ZnO, were assigned to donor bound excitons.

Acknowledgments

The work of A. V. Rodina was carried out during the stay at the Institute for Solid State Physics, TU Berlin, and supported by the Deutsche Forschungsgemeinschaft (DFG).

* permanent address: A. F. Ioffe Physico-Technical Institute, 194021, St.-Petersburg, Russia.

¹ J. Gutowski, N. Presser, I. Broser, Phys. Rev. **B 38**, 9746 (1988).

² G. Blattner, C. Klingshirn, R. Helbig, R. Meinl, phys. stat. sol. (b) **107**, 105 (1981).

³ P. Loose, M. Rosenzweig, M. Wöhlecke, phys. stat. sol. (b) **75**, 137 (1976).

⁴ D.C. Reynolds, C.W. Litton, T.C. Collins, Phys. Rev. **140**, A1726 (1965).

⁵ D. C. Reynolds and T.C. Collins, Phys. Rev. **185**, 1099 (1969).

⁶ K. Thonke, Th. Gruber, N. Teofilov, R. Schönfelder, A. Waag, and R. Sauer, Physica **B 308-310**, 945 (2001).

⁷ K. Thonke, N. Kerwien, A. Wyszomolek, M. Potemski, A. Waag, and R. Sauer, Mat. Res. Soc. Symp. Proc. Vol. 719, F2.4.1 (2002); K. Thonke, N. Kerwien, A. Wyszomolek, M. Potemski, A. Waag, and R. Sauer, in Proc. 26th Int'l Conf. on the Physics of Semiconductors, edited by A. R. Long

and J. H. Davies, Institute of Physics Publishing, Bristol (UK) and Philadelphia (USA), Institute of Physics Conference Series Number **171**, P22, (2003).

⁸ A. Zeuner, H. Alves, D. M. Hoffman, B. K. Meyer, M. Heuken, J. Blasing, and A. Krost, Appl. Phys. Lett. **80**, 2078 (2002).

⁹ J.L. Birman, Phys. Rev. **114**, 1490 (1959).

¹⁰ J.J. Hopfield, J. Phys. Chem. Solids **15**, 97 (1960).

¹¹ D.G. Thomas, J. Phys. Chem. **15**, 86 (1960).

¹² Y. S. Park, C. W. Litton, T. C. Collins, and D. C. Reynolds, Phys. Rev. **143**, 512 (1966).

¹³ B. Segall, Phys. Rev. **163**, 769 (1967).

¹⁴ W. Y. Liang and A. D. Yoffe, Phys. Rev. Lett. **20**, 59 (1968).

¹⁵ K. Hümmer, Phys. Stat. Sol. **56**, 249 (1973).

¹⁶ M. Rosenzweig, Diploma Thesis, TU Berlin, 1975.

¹⁷ G. Blattner, G. Kurtze, G. Schmieder, and C. Klingshirn, Phys. Rev. **B 25**, 7413 (1982).

¹⁸ B. Gil, Phys. Rev. **B 64**, 201310(R) (2001); B. Gil, A.

- Lusson, V. Sallet, R. Triboulet, and P. Bigenwald, *Jpn. J. Appl. Phys. Lett.* **40**, L1089 (2001).
- ¹⁹ D. C. Reynolds, D. C. Look, B. Jogai, C. W. Litton, G. Cantwell, and W. C. Harsch, *Phys. Rev.* **B 60**, 2340 (1999).
 - ²⁰ W. R. L. Lambrecht, A. V. Rodina, S. Limpijumnong, B. Segall, and B. K. Meyer, *Phys. Rev.* **B 65**, 075207 (2002).
 - ²¹ D.G. Thomas, J.J. Hopfield, *Phys. Rev.* **128**, 2135 (1962).
 - ²² H. Alves, D. Pfisterer, A. Zeuner, T. Riemann, J. Christen, D. M. Hofmann, and B. K. Meyer, *Optical Materials* **23**, 33 (2003).
 - ²³ B. K. Meyer, H. Alves, D. M. Hofman, W. Kriegseis, T. Riemann, J. Christen, A. Hoffmann, M. Strassburg, M. Dworzak, U. Haboeck, and A. V. Rodina, to be published in *phys. stat. sol. (b)*.
 - ²⁴ The notation for the hole g factor and the order of the hole Zeeman split components is the same as in Ref. 20
 - ²⁵ T. Skettrup, M. Suffczynski, and W. Gorzkowski, *Phys. Rev.* **B 4**, 512 (1971).
 - ²⁶ M. A. Lampert, *Phys. Rev. Lett.* **1**, 450 (1958).
 - ²⁷ A. Zeuner, H.R. Alves, D.M. Hofmann, B.K. Meyer, A. Hoffmann, U. Haboeck, M. Straburg, M. Dworzak, *phys. stat. sol. (b)* **234**, R7-R9 (2002).
 - ²⁸ This value can be calculated using the theory developed in Ref. 35 with effective mass Luttinger parameters from Ref. 20.
 - ²⁹ D. M. Hofmann, A. Hofstaetter, F. Leiter, H. Zhou, F. Henecker, B. K. Meyer, S. B. Orlinskii, J. Schmidt, and P. G. Baranov, *Phys. Rev. Lett.* **88**, 045504 (2002).
 - ³⁰ M. Strassburg, A. V. Rodina, M. Dworzak, U. Haboeck, A. Hoffmann, A. Zeuner, H. R. Alves, D. M. Hofmann, and B. K. Meyer, to be published in *Appl. Phys. Lett.*
 - ³¹ E. Tomzig and R. Helbig, *J. of Luminescence* **14**, 403 (1976).
 - ³² A. Kaschner, U. Haboeck, Martin Strassburg, Matthias Strassburg, G. Kaczmarczyk, A. Hoffmann, C. Thomsen, A. Zeuner, H.R. Alves, D.M. Hofmann, B.K. Meyer, *Appl. Phys. Lett.* **80**, 1909 (2002).
 - ³³ Martin Strassburg, U. Haboeck, A. Kaschner, Matthias Strassburg, A.V. Rodina, A. Hoffmann, C. Thomsen, A. Zeuner, H.R. Alves, D.M. Hofmann, B.K. Meyer, in *Proc. 26th Int'l Conf. on the Physics of Semiconductors*, edited by A. R. Long and J. H. Davies, Institute of Physics Publishing, Bristol (UK) and Philadelphia (USA), Institute of Physics Conference Series Number **171**, P45, (2003).
 - ³⁴ H.-C. Pan, B. W. Wessels, *Mat. Res. Soc. Symp. Proc. Vol.* **152**, 219 (1989).
 - ³⁵ A. V. Malyshev, I. A. Merkulov, and A. V. Rodina, *Fiz. Tverd. Tela* **40**, 1002 (1998) [*Physics of the Solid State* **40**, 917 (1998)].

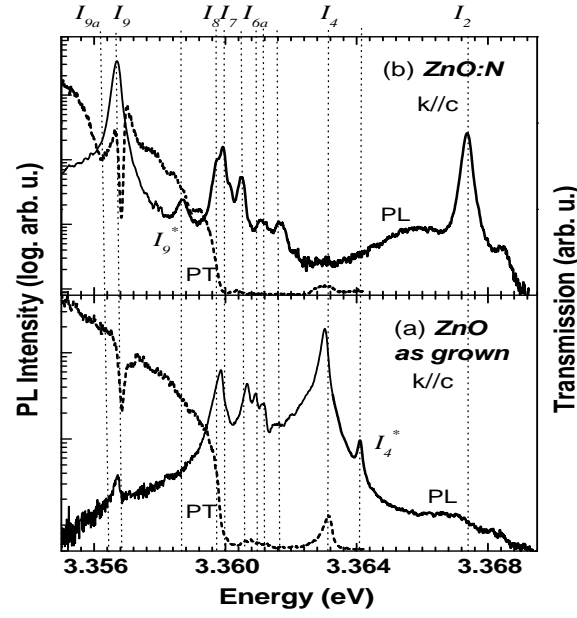


FIG. 1: Photoluminescence (solid lines) and transmission (dashed lines) spectra of the undoped as grown ZnO (a) and nitrogen doped ZnO:N (b) at 4.2 K

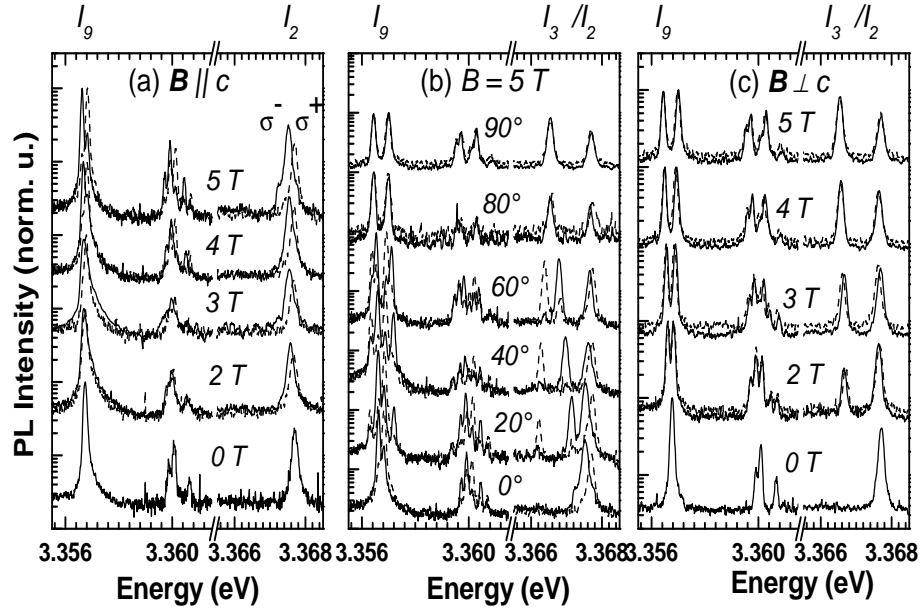


FIG. 2: Photoluminescence spectra of ZnO:N at 4.2 K for different magnetic fields in (a) Faraday configuration ($B \parallel c$ and $k \parallel c$), (c) Voigt configuration ($B \perp c$ and $k \parallel c$), and for the different angles Θ between c axis and magnetic field direction B at 5 T. The spectra measured for right polarized light σ^+ and left polarized light σ^- are shown by dashed and solid lines, respectively.

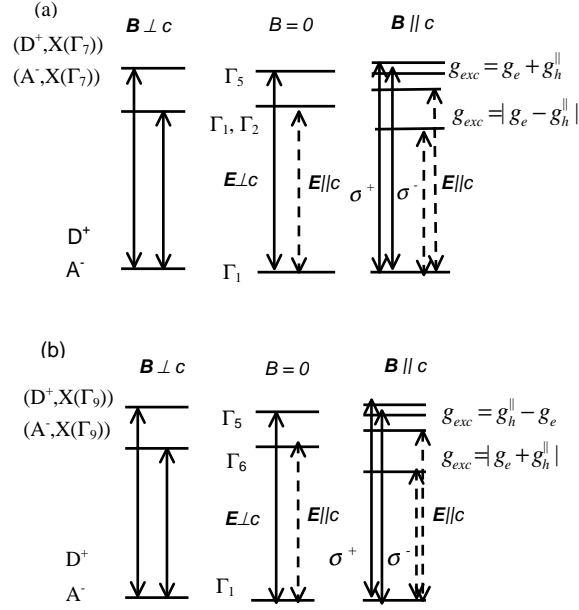


FIG. 3: Level schemes of ionized bound exciton transitions. Case(a): an exciton involving a hole of Γ_7 symmetry, and case (b): an exciton involving a hole of Γ_9 symmetry. Note that in (b) the transitions with $\mathbf{E} \parallel c$ are first forbidden but might be observed due to high-order perturbations.

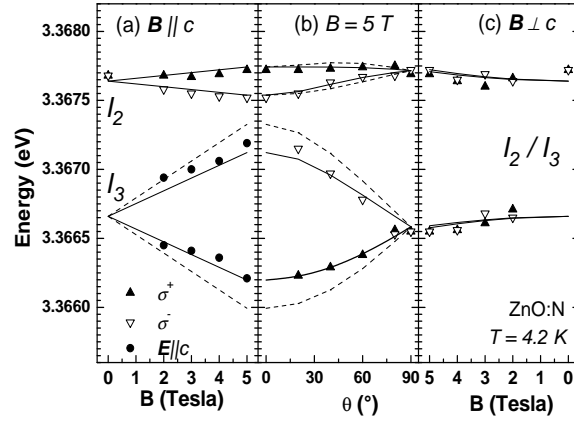


FIG. 4: Zeeman splitting of the bound exciton line I_2 for $\mathbf{B} \parallel c$ (a), $\mathbf{B} \perp c$ (c) and its angular dependence for $B = 5 T$ (b). Symbols are experimental data, lines are fits for the transitions allowed with circular polarized light (σ^+ or σ^-) and linear polarized light ($\mathbf{E} \parallel c$), respectively. The hole is assumed to be of Γ_7 symmetry with $|g_h^{\parallel}| < g_e$ (solid lines) and of Γ_9 symmetry with $|g_h^{\parallel}| > g_e$ (dashed lines).

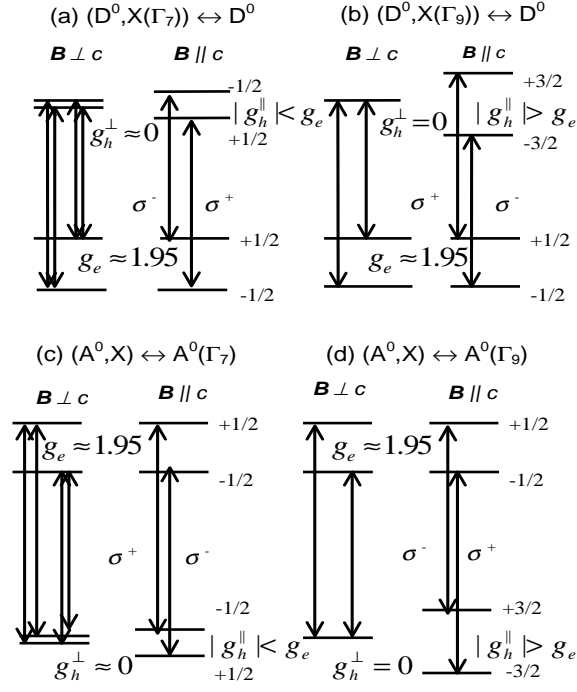


FIG. 5: Level schemes of neutral bound exciton transitions. Cases (a) and (b): donor bound excitons involving a hole of Γ_7 symmetry and of Γ_9 symmetry, respectively. Cases (c) and (d): acceptor bound excitons involving a hole of Γ_7 symmetry and of Γ_9 symmetry, respectively.

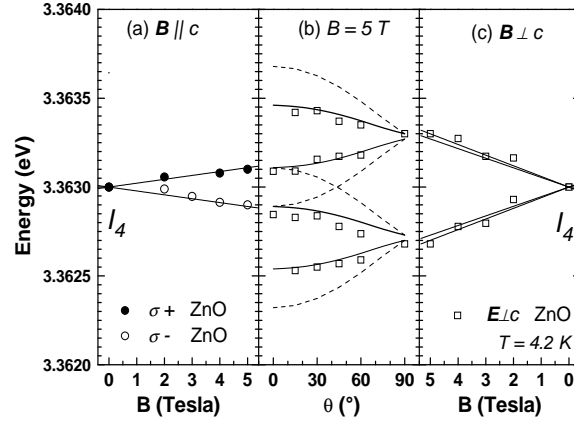


FIG. 6: Zeeman splitting of the bound exciton line I_4 for $B \parallel c$ (a), $B \perp c$ (c) and its angular dependence for $B = 5$ T (b). Symbols are experimental data and lines are fits for the transitions allowed for circular polarized light (σ^+ or σ^-). The hole is assumed to be of Γ_7 symmetry with $|g_h^{\parallel}| < g_e$ (solid lines) and of Γ_9 symmetry with $|g_h^{\parallel}| > g_e$ (dashed lines).

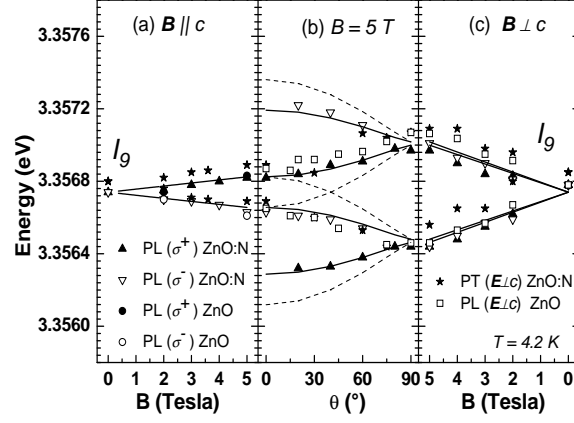


FIG. 7: Zeeman splitting of the bound exciton line I_9 for $B \parallel c$ (a), $B \perp c$ (c) and its angular dependence for $B = 5$ T (b). Symbols are experimental data and lines are fits for the transitions allowed for circular polarized light (σ^+ or σ^-). The hole is assumed to be of Γ_7 symmetry with $|g_h^{\parallel}| < g_e$ (solid lines) and of Γ_9 symmetry with $|g_h^{\parallel}| > g_e$ (dashed lines).

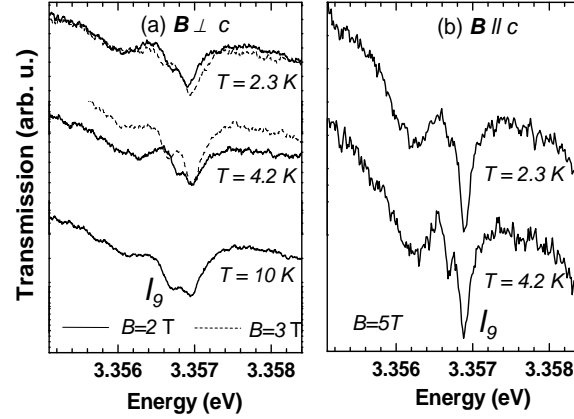


FIG. 8: Temperature-dependent transmission spectra of the bound exciton line I_9 in ZnO:N for magnetic field $B = 2$ T (solid curve) and $B = 3$ T (dashed curve) perpendicular to the c axis of the crystal (a) and magnetic field $B = 5$ T parallel to the c axis of the crystal (b).

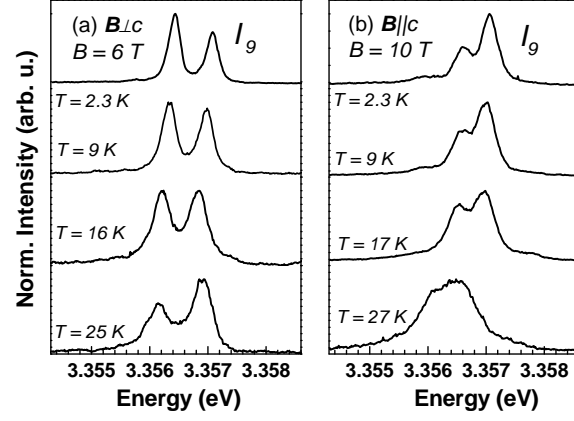


FIG. 9: Temperature-dependent PL spectra of the bound exciton line I_9 in ZnO:N for magnetic field $B = 6$ T perpendicular to the c axis of the crystal (a) and magnetic field $B = 10$ T parallel to the c axis of the crystal (b). Note that the spectral resolution in (a) and (b) is limited to 0.3 meV.

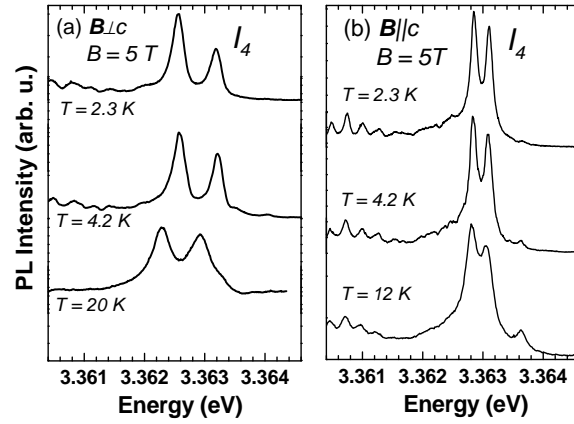


FIG. 10: Temperature-dependent PL spectra of the bound exciton line I_4 in as grown ZnO for magnetic field $B = 5$ T perpendicular to the c axis of the crystal (a) and parallel to the c axis of the crystal (b).